

Supporting information for: Solvent effects on excited-state structures: A quantum Monte Carlo and density functional study

Riccardo Guareschi,[†] Franca Maria Floris,^{*,‡} Claudio Amovilli,^{*,‡} and Claudia
Filippi^{*,†}

*MESA+ Institute for Nanotechnology, University of Twente, P.O. Box 217, 7500 AE Enschede,
The Netherlands, and Dipartimento di Chimica e Chimica Industriale, Università di Pisa, Via
Risorgimento 35, 56126 Pisa, Italy*

E-mail: floris@dcci.unipi.it; amovilli@dcci.unipi.it; c.filippi@utwente.nl

*To whom correspondence should be addressed

[†]MESA+ Institute for Nanotechnology, University of Twente, P.O. Box 217, 7500 AE Enschede, The Netherlands

[‡]Dipartimento di Chimica e Chimica Industriale, Università di Pisa, Via Risorgimento 35, 56126 Pisa, Italy

All bond lengths and atomic coordinates are given in Angstrom (\AA) and all bond angles are given in degrees ($^\circ$). All the structural parameters are optimized in the presence of PCM water ($\epsilon = 78.39$). The radii of the spheres used to build the PCM cavities for the different molecules are also reported in Angstrom (\AA).

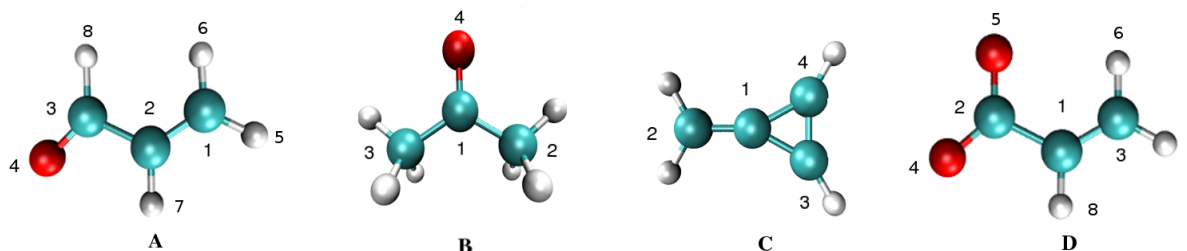


Figure S1: Molecules with labels: **A**) *s*-trans acrolein, **B**) acetone, **C**) methylenecyclopropene (MCP), and **D**) the propenoic acid anion (PAA).

1 Basis-set convergence

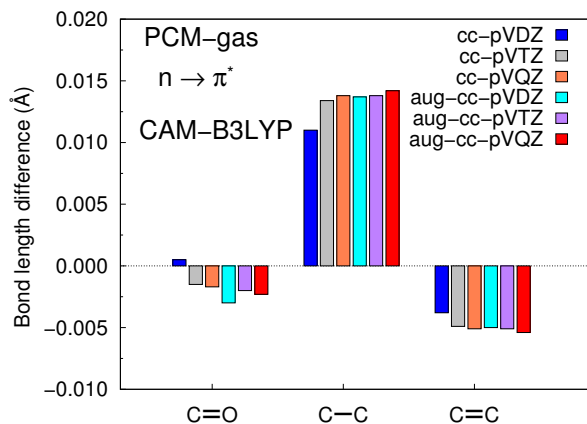


Figure S2: Convergence with basis set of the bond-length differences between PCM and gas phase for the $n \rightarrow \pi^*$ state of *s*-trans acrolein at the TDDFT/CAM-B3LYP level.

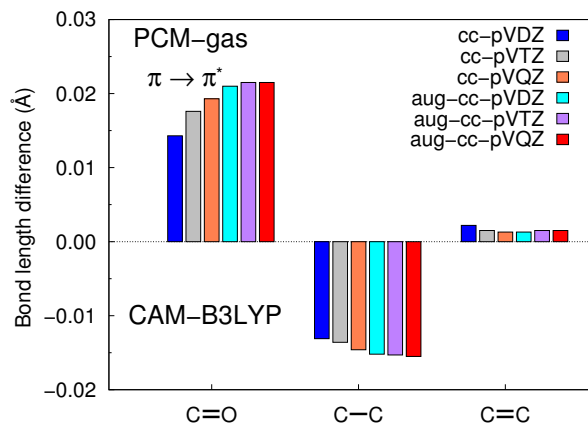


Figure S3: Convergence with basis set of the bond-length differences between PCM and gas phase for the $\pi \rightarrow \pi^*$ state of *s*-trans acrolein at the TDDFT/CAM-B3LYP level.

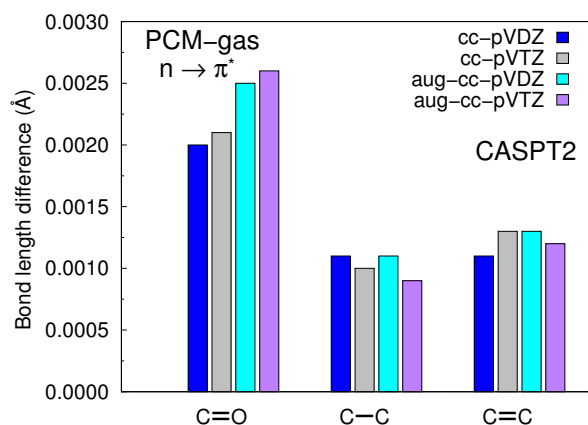


Figure S4: Convergence with basis set of the bond-length differences between PCM and gas phase for the $n \rightarrow \pi^*$ state of *s*-trans acrolein at the CASPT2 level.

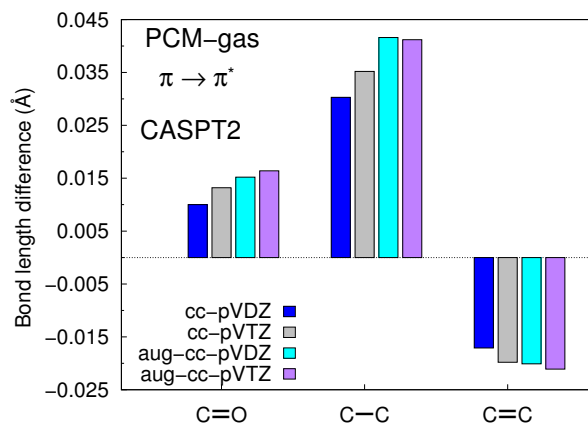


Figure S5: Convergence with basis set of the bond-length differences between PCM and gas phase for the $\pi \rightarrow \pi^*$ state of *s*-trans acrolein at the CASPT2 level. The CASPT2 geometries are obtained with a sub-optimal CAS(2,2) active space (see text).

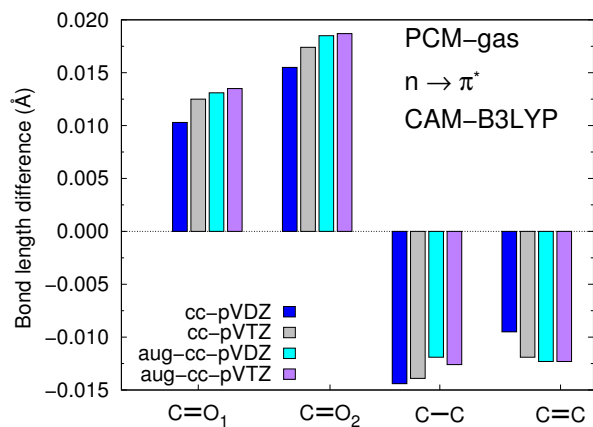


Figure S6: Convergence with basis set of the bond-length differences between PCM and gas phase for the $n \rightarrow \pi^*$ state of PAA at the TDDFT/CAM-B3LYP level.

2 Dependence on the PCM cavity parameters

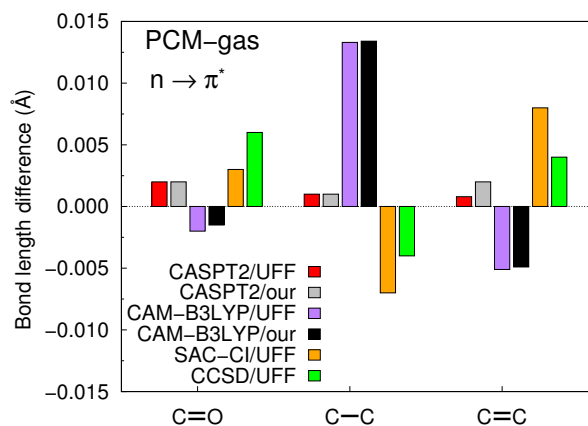


Figure S7: Bond-length differences between PCM and gas phase computed with different sets of spheres for the $n \rightarrow \pi^*$ state of *s*-trans acrolein. “our” is the set of spheres whose radii are listed in the following Section and UFF is the Universal Force Field set. We use the cc-pVTZ basis set for the CASPT2 and TDDFT/CAM-B3LYP calculations. The SAC-CI and CCSD values are taken from Ref. 15 and Ref. 17, respectively.

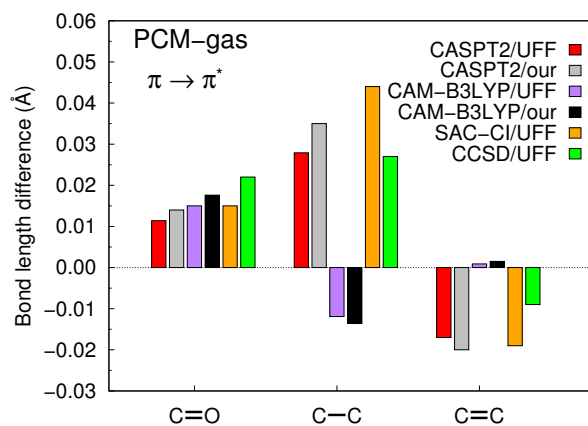


Figure S8: Bond-length differences between PCM and gas phase computed with different sets of spheres for the $\pi \rightarrow \pi^*$ state of *s*-trans acrolein (“our” is the set of spheres whose radii are listed in the following Section and UFF is the Universal Force Field set). We use the cc-pVTZ basis set for the CASPT2 and TDDFT/CAM-B3LYP calculations. The SAC-CI and CCSD values are taken from Ref. 15 and Ref. 17, respectively. The CASPT2 geometries are obtained with a sub-optimal CAS(2,2) active space (see text).

3 *s*-trans acrolein in PCM water

Table S1: Radii of the spheres centered on the different atoms of *s*-trans acrolein.

C ₁	2.021
C ₂	2.021
C ₃	1.984
O ₄	1.805
H ₅	1.391
H ₆	1.381
H ₇	1.376
H ₈	1.450

Table S2: TDDFT, CASPT2, and VMC bond lengths and angles of *s*-trans acrolein in the $n \rightarrow \pi^*$ and $\pi \rightarrow \pi^*$ excited states ($1^1A''$ and $2^1A'$, respectively).

	B3LYP	CAM-B3LYP	PBE0	M06	M06-2X	CASPT2	VMC
	$1^1A'', n \rightarrow \pi^*$						
C=O	1.286	1.277	1.276	1.274	1.274	1.338	1.330(0)
C–C	1.393	1.417	1.396	1.395	1.433	1.378	1.372(0)
C=C	1.375	1.349	1.369	1.363	1.345	1.394	1.387(0)
$\theta(\text{C–C–C})$	124.22	124.25	124.22	124.16	123.85	123.00	123.05(2)
$\theta(\text{C–C–O})$	128.89	126.82	129.13	129.53	125.80	124.09	124.87(3)
	$2^1A', \pi \rightarrow \pi^*$						
C=O	1.269	1.262	1.263	1.253	1.265	1.293	1.290(0)
C–C	1.443	1.422	1.436	1.434	1.420	1.479	1.460(0)
C=C	1.451	1.457	1.450	1.453	1.461	1.409	1.424(0)
$\theta(\text{C–C–C})$	126.95	125.82	126.66	125.98	125.13	128.92	126.27(12)
$\theta(\text{C–C–O})$	121.28	121.93	121.41	121.94	122.14	117.98	119.34(5)

Table S3: VMC bond lengths and angles of *s*-trans acrolein in the $n \rightarrow \pi^*$ excited state ($1^1A''$) optimized with a two-body and a three-body Jastrow factor.

VMC	$1^1A'', n \rightarrow \pi^*$	
GAS	\mathcal{I}_{ab}	\mathcal{I}_{abc}
C=O	1.327(0)	1.327(1)
C–C	1.368(0)	1.372(0)
C=C	1.383(0)	1.389(1)
$\theta(C-C-C)$	122.57(1)	122.57(1)
$\theta(C-C-O)$	125.82(1)	125.82(1)
PCM	\mathcal{I}_{ab}	\mathcal{I}_{abc}
C=O	1.330(0)	1.330(0)
C–C	1.368(0)	1.372(0)
C=C	1.382(0)	1.387(0)
$\theta(C-C-C)$	123.00(2)	123.05(2)
$\theta(C-C-O)$	125.09(2)	124.87(3)

Table S4: VMC bond lengths and angles of *s*-trans acrolein in the $\pi \rightarrow \pi^*$ excited state ($2^1A'$) optimized with a two-body and a three-body Jastrow factor.

VMC	$2^1A', \pi \rightarrow \pi^*$	
GAS	\mathcal{I}_{ab}	\mathcal{I}_{abc}
C=O	1.266(2)	1.259(0)
C–C	1.443(1)	1.456(0)
C=C	1.428(1)	1.430(0)
$\theta(C-C-C)$	123.92(6)	123.92(6)
$\theta(C-C-O)$	121.64(1)	121.64(1)
PCM	\mathcal{I}_{ab}	\mathcal{I}_{abc}
C=O	1.289(1)	1.290(0)
C–C	1.457(1)	1.460(0)
C=C	1.418(1)	1.422(0)
$\theta(C-C-C)$	126.31(24)	126.31(24)
$\theta(C-C-O)$	118.97(18)	118.97(18)

Table S5: CASPT2 bond lengths and angles of *s*-trans acrolein in the $\pi \rightarrow \pi^*$ excited state ($2^1A'$) optimized with different active spaces at the single-state and multistate CASPT2 level.

CASPT2	$2^1A', \pi \rightarrow \pi^*$	
CAS(2,2)	SS	MS
C=O	1.303	1.293
C–C	1.487	1.479
C=C	1.410	1.409
$\theta(\text{C–C–C})$	128.13	128.92
$\theta(\text{C–C–O})$	116.50	117.98
CAS(4,4)		
C=O	1.346	1.292
C–C	1.402	1.509
C=C	1.427	1.506
$\theta(\text{C–C–C})$	122.78	128.78
$\theta(\text{C–C–O})$	121.66	115.52

Table S6: XYZ coordinates of the optimized VMC/PCM geometry of the $n \rightarrow \pi^*$ ($1^1A''$) state of *s*-trans acrolein optimized in the planar C_s conformation. We employ a CAS(6,5) expansion and the cc-pVTZ' basis set in combination with a three-body Jastrow factor.

C	-1.97670	0.62291	0.00000
C	-1.06303	1.66731	0.00000
C	0.29566	1.47389	0.00000
O	1.20366	2.44969	0.00000
H	-3.02909	0.82301	0.00000
H	-1.64690	-0.40092	0.00000
H	-1.42413	2.68255	0.00000
H	0.75034	0.49109	0.00000

Table S7: XYZ coordinates of the optimized VMC/PCM geometry of the $\pi \rightarrow \pi^*$ ($2^1A'$) state of *s*-trans acrolein optimized in the planar C_s conformation. We employ a CAS(4,4) expansion and the cc-pVTZ' basis set in combination with a three-body Jastrow factor.

C	-1.97558	0.62596	0.00000
C	-1.03336	1.69278	0.00000
C	0.42290	1.58314	0.00000
O	1.12570	2.66461	0.00000
H	-3.02807	0.84441	0.00000
H	-1.63806	-0.39788	0.00000
H	-1.44339	2.69441	0.00000
H	0.86961	0.59651	0.00000

4 Acetone in PCM water

Table S8: Radii of the spheres centered on the different atoms of acetone.

C ₁	1.984
C ₂	2.021
C ₃	2.021
O ₄	1.805
H	1.391

Table S9: TDDFT, CASPT2, and VMC bond lengths and angles of acetone in the $n \rightarrow \pi^*$ excited state in two different conformations (planar C_{2v} and pyramidalized C_s).

	B3LYP	CAM-B3LYP	PBE0	M06	M06-2X	CASPT2	VMC
	$1^1A_2 (C_{2v})$						
C=O	1.322	1.304	1.312	1.311	1.293	1.363	1.354(1)
C-C	1.498	1.501	1.493	1.488	1.513	1.487	1.490(1)
$\theta(C-C-O)$	117.95	118.36	118.09	118.29	119.25	116.73	118.97(1)
	$1^1A'' (C_s)$						
C=O	1.307	1.292	1.299	1.298	1.283	1.353	1.349(0)
C-C	1.512	1.512	1.505	1.501	1.526	1.497	1.499(0)
$\theta(C-C-O)$	114.68	114.81	114.80	114.72	115.05	112.68	115.50(43)
$\Theta(H-C-C-O)$	52.03	52.11	51.92	52.28	51.04	52.24	50.21(6)

Table S10: VMC bond lengths and angles of acetone in the $n \rightarrow \pi^*$ excited state in the C_{2v} conformation (1^1A_2) optimized with a two-body and a three-body Jastrow factor.

VMC	$1^1A_2, n \rightarrow \pi^*$	
GAS	\mathcal{I}_{ab}	\mathcal{I}_{abc}
C=O	1.348(1)	1.350(0)
C-C	1.481(1)	1.490(1)
$\theta(C-C-O)$	118.99(4)	118.99(4)
PCM	\mathcal{I}_{ab}	\mathcal{I}_{abc}
C=O	1.348(0)	1.354(1)
C-C	1.481(0)	1.490(1)
$\theta(C-C-O)$	118.97(1)	118.97(1)

Table S11: VMC bond lengths and angles of acetone in the $n \rightarrow \pi^*$ excited state in the C_s conformation ($1^1A''$) optimized with a two-body and a three-body Jastrow factor.

VMC	$1^1A'', n \rightarrow \pi^*$	
	\mathcal{J}_{ab}	\mathcal{J}_{abc}
GAS		
C=O	1.344(1)	1.346(0)
C-C	1.489(1)	1.499(0)
$\theta(\text{C-C-O})$	112.52(8)	112.52(8)
$\Theta(\text{H-C-C-O})$	52.16(13)	52.16(13)
PCM		
C=O	1.343(0)	1.349(0)
C-C	1.490(0)	1.499(0)
$\theta(\text{C-C-O})$	112.74(0)	115.50(43)
$\Theta(\text{H-C-C-O})$	50.76(1)	50.21(6)

Table S12: XYZ coordinates of the optimized VMC/PCM geometry of the $n \rightarrow \pi^*$ (1^1A_2) state of acetone in the planar C_{2v} conformation. We employ a CAS(4,3) expansion and the cc-pVTZ' basis set in combination with a three-body Jastrow factor.

C	0.00000	0.00000	0.13241
C	0.00000	1.29776	-0.59350
C	0.00000	-1.32264	-0.55400
O	-0.00105	0.00656	1.48777
H	0.87351	1.39431	-1.22768
H	-0.87493	1.39450	-1.22847
H	0.87515	-1.43169	-1.18295
H	-0.87602	-1.42166	-1.18491
H	-0.01014	2.12566	0.09945
H	-0.00670	-2.13946	0.15399

Table S13: XYZ coordinates of the optimized VMC/PCM geometry of the $n \rightarrow \pi^*$ ($1^1A''$) state of acetone in the pyramidalized C_s conformation. We employ a CAS(4,3) expansion and the cc-pVTZ' basis set in combination with a three-body Jastrow factor.

C	0.14183	0.15352	0.00000
C	0.08387	-0.58300	1.29457
C	0.08359	-0.58659	-1.29239
O	-0.60879	1.26696	-0.00524
H	0.81055	-1.38093	1.28249
H	0.81659	-1.37830	-1.27650
H	0.30732	0.06779	2.12688
H	0.29697	0.06891	-2.12428
H	-0.90326	-1.00833	1.45471
H	-0.90067	-1.01909	-1.45072

5 Methylenecyclopropene in PCM water

Table S14: Radii of the spheres centered on the different atoms of methylenecyclopropene.

C	2.021
H	1.391

Table S15: TDDFT, CASPT2, and VMC bond lengths and angles of methylenecyclopropene in the $\pi \rightarrow \pi^*$ excited state optimized in the planar C_{2v} conformation.

	B3LYP	CAM-B3LYP	PBE0	M06	M06-2X	CASPT2	VMC
	$1^1B_2 (C_{2v})$						
$C_1=C_2$	1.425	1.401	1.418	1.413	1.406	1.459	1.456(0)
C_1-C_3	1.357	1.354	1.357	1.353	1.357	1.362	1.356(0)
$C_4=C_3$	1.497	1.491	1.490	1.478	1.488	1.496	1.487(0)
$\theta(C_2-C_1-C_3)$	146.51	146.60	146.71	146.87	146.77	146.99	146.74(1)

Table S16: VMC bond lengths and angles of methylenecyclopropene in the $\pi \rightarrow \pi^*$ excited state optimized in the planar C_{2v} conformation with a two-body and a three-body Jastrow factor.

VMC	$1^1B_2, \pi \rightarrow \pi^*$	
GAS	\mathcal{I}_{ab}	\mathcal{I}_{abc}
$C_1=C_2$	1.456(1)	1.459(0)
C_1-C_3	1.351(1)	1.353(0)
$C_4=C_3$	1.483(0)	1.485(0)
$\theta(C_2-C_1-C_3)$	146.66(2)	146.66(2)
PCM	\mathcal{I}_{ab}	\mathcal{I}_{abc}
$C_1=C_2$	1.455(0)	1.456(0)
C_1-C_3	1.353(0)	1.356(0)
$C_4=C_3$	1.482(0)	1.487(0)
$\theta(C_2-C_1-C_3)$	146.75(0)	146.74(1)

Table S17: XYZ coordinates of the optimized VMC/PCM geometry of the $\pi \rightarrow \pi^*$ (1^1B_2) state of methylenecyclopropene in the C_{2v} conformation. We employ a CAS(4,4) expansion and the cc-pVTZ' basis set in combination with a three-body Jastrow factor.

C	0.00000	0.00000	-0.13153
C	0.00000	0.00000	1.32430
C	0.00000	0.74360	-1.26514
C	0.00000	-0.74384	-1.26496
H	0.00000	0.93061	1.85873
H	0.00000	-0.92994	1.86003
H	0.00000	1.68089	-1.76982
H	0.00000	-1.67958	-1.77363

6 Propenoic acid anion in PCM water

Table S18: Radii of the spheres centered on the different atoms of propenoic acid anion.

C ₁	2.021
C ₂	1.937
C ₃	2.021
O ₄	1.831
H ₅	1.799
H ₆	1.381
H ₇	1.392
H ₈	1.376

Table S19: TDDFT, CASPT2, and VMC bond lengths and angles of the propenoic acid anion in the $n \rightarrow \pi^*$ excited state optimized in the planar C_s conformation.

	B3LYP	CAM-B3LYP	PBE0	M06	M06-2X	CASPT2	VMC
	$1^1A'' (C_s)$						
C–O ₄	1.295	1.292	1.290	1.287	1.301	1.300	1.298(0)
C–O ₅	1.301	1.303	1.296	1.295	1.305	1.297	1.297(0)
C–C	1.395	1.389	1.393	1.389	1.396	1.385	1.382(0)
C=C	1.406	1.384	1.401	1.398	1.378	1.407	1.408(0)
$\theta(O_4-C-C)$	124.50	124.43	124.34	123.70	124.96	124.70	124.27(4)
$\theta(C-C-C)$	127.81	128.69	128.00	128.34	128.00	130.89	127.20(2)
$\theta(O_4-C-O_5)$	105.77	106.15	105.61	105.66	106.35	100.00	107.27(4)

Table S20: VMC bond lengths and angles of propenoic acid anion in the $n \rightarrow \pi^*$ excited state ($1^1A''$) optimized with a two-body and a three-body Jastrow factor.

VMC	$1^1A'', n \rightarrow \pi^*$	
	\mathcal{J}_{ab}	\mathcal{J}_{abc}
GAS		
C–O ₄	1.291(1)	1.293(0)
C–O ₅	1.284(1)	1.297(0)
C–C	1.379(0)	1.385(0)
C=C	1.401(0)	1.408(0)
$\theta(O_4-C-C)$	128.33(7)	128.33(7)
$\theta(C-C-C)$	124.49(7)	124.49(7)
$\theta(O_4-C-O_5)$	107.18(7)	107.18(7)
PCM		
C–O ₄	1.292(0)	1.298(0)
C–O ₅	1.290(0)	1.297(0)
C–C	1.378(0)	1.382(0)
C=C	1.402(0)	1.408(0)
$\theta(O_4-C-C)$	124.27(4)	124.27(4)
$\theta(C-C-C)$	127.20(2)	127.20(2)
$\theta(O_4-C-O_5)$	107.27(4)	107.27(4)

Table S21: XYZ coordinates of the optimized VMC/PCM geometry of the $n \rightarrow \pi^*$ ($1^1A''$) state of propenoic acid anion in the planar C_s conformation. We employ a CAS(10,7) expansion and the cc-pVTZ' basis set in combination with a three-body Jastrow factor.

C	-0.59194	-0.78457	0.00000
C	-0.09434	0.50377	0.00000
C	0.20824	-1.94437	0.00000
O	1.15483	0.85776	0.00000
O	-0.75827	1.61687	0.00000
H	1.27748	-1.87533	0.00000
H	-0.23613	-2.91969	0.00000
H	-1.66484	-0.86181	0.00000